Insights into the degradation of diphenhydramine – An emerging SARS-CoV-2 medicine by UV/Sulfite

Hiu Lam So [a], Liwen Wang [b], Jianghui Liu [a], Wei Chu [a,*], Tao Li [c], Amal Abdelhaleem [d,*]

[a] *Department of Civil and Environmental Engineering, The Hong Kong Polytechnic University, Hung Hom, Hong Kong*
[b] *Department of Civil and Environmental Engineering, University of California, Berkeley, 760 Davis Hall, Berkeley, CA 94720, United States*
[c] *Department of Civil and Environmental Engineering, The Hong Kong University of Science and Technology, Clear Water Bay, Kowloon, Hong Kong*
[d] *Environmental Engineering Department, Egypt-Japan University of Science and Technology, New Borg El-Arab City, Alexandria 21934, Egypt*

ABSTRACT

As Diphenhydramine (DPH) has been considered as a drug to treat SARS-CoV-2, the degradation of DPH from water was investigated and evaluated in this study by adopting an advanced oxidation/advanced reduction process – the UV/sulfite process. The UV/sulfite system was able to eliminate DPH within 6 mins under UV_{254nm} and 1.0 mM sulfite. It was observed that the presence of NO_3^-, NO_2^-, Cl^-, HCO_3^-, and SO_4^{2-} anions in water can affect the performance of UV/Sulfite degradation system. The mechanism of UV/sulfite/anions was evaluated which the presence of NO_3^- in UV/sulfite process has revealed faster initial decay rate but lower final DPH removal. It was observed that the UV/Sulfite process was extremely sensitive to pH as the dissociation of ion species varied among pH. The reaction became sluggish in acidic solution due to the dissociation of less reactive species such as HSO_3. In alkaline solution, SO_3^{2-} was the dominant species, producing powerful $SO_3^{\bullet-}$ and e_{aq}^- when activated by UV at 254 nm. By conducting LC/MS analysis, the degradation pathway was proposed and can be summarized into four main pathways: hydroxylation, side chain cleavage, losing aromatic ring or ring opening. Scavenging tests were also carried out and validated the presence of various radicals contributing to the reaction, including e_{aq}^-, H, OH, SO_3^-, $O_2^{\bullet-}$ and SO_4^-.

1. Introduction

The COVID-19 caused by SARS-CoV-2 has led to a global health concern and safe drugs for prevention have been an urge to for protecting vulnerable populations. It has been reported that antihistamine has a high potential to alleviate the symptoms caused by SARS-CoV-2 [1]. Diphenhydramine - a widely used over-the-counter antihistamine as the form of diphenhydramine hydrochloride (DPH) to relieve symptoms of allergy and common cold, has been discovered by an *in vitro* study to exhibit direct antiviral property against SARS-CoV-2 and the usage of diphenhydramine can reduce the positivity of SARS-CoV-2 in older subjects [2]. With the hope of using diphenhydramine for disease prevention, early intervention or therapy of COVID-19, extensive use of diphenhydramine could cause disaster to the aquatic ecosystem when discharged if they are not treated correspondingly. Although the detected concentration of pharmaceuticals and personal care products (PPCPs) are relatively low (less than 1 μg/L) [3], they are persistent in the environment and can affect the metabolisms and biology of most aquatic lives. It has been reported that around 2–15 % of DPH are excreted unmetabolized and the removal of antihistamines like DPH in municipal wastewater treatment plants is only 69 % [4]. Among many

kinds of pharmaceuticals discharged to the environment, DPH is one of them that has been specifically identified in major streams 0.01 to 0.10 μg/L [5,6], soil (20 – 50 μg/kg) [6], and fish tissue in multiple studies [7–9]. According to Du, Price, Scott, Kristofco, Ramirez, Chambliss, Yelderman and Brooks [4], the *n*-octanol water partition coefficient of DPH ($logK_{ow}$ = 3) was significantly higher among other water contaminants and the presence of DPH in municipal wastewater influence has exhibited huge seasonal difference which the concentration was significantly greater in fall (530 to 600 μg/L) then winter (160 to 180 μg/L).

The exposure of streams ecosystems to DPH can cause a reduction of 61 % in respiration and 99 % in photosynthesis [3]. It has been found that DPH could be photodegraded under sunlight in the presence of humic substances with half-lives of 5.4 h and is inactivated in 200 days using anaerobic biological treatment [10,11]. In order to facilitate DPH removal in wastewater treatment plant, a more efficient method is proposed for DPH removal.

Previous studies of DPH removal in different photo-reactors by UV-C/H_2O_2 showed that total removal can be achieved under 150 mg/L of H_2O_2 in 60 min, while only 10 % of Total Organic Carbon (TOC) was removed [12]. Fenton process is also a common process to remove such

pharmaceuticals in wastewater. It is reported that in dosages of 15 mg/L and 2.5 mg/L of H_2O_2 and Fe^{2+}, 60 % of DPH is removed in 60 min, where the removal was increased with increasing dosages of reactants [12]. However, such total removal required excessive dosage of H_2O_2 and Fe^{2+}, which could generate secondary pollution in effluent. Therefore, heterogeneous catalysis for DPH removal was considered. TiO_2 with UV-A was studied and around 50 % removal was achieved [12]; Adsorption of DPH was studied on swelling clay, activated carbon and aluminosilicates [13–15]. However, the adsorption process is rather slow, often required several hours to reach the equilibrium. To achieve faster reaction and better removal, advanced oxidation and reduction were examined.

Sulfate radicals ($SO_4^{\cdot-}$) and hydroxyl radicals ($\cdot OH$) have been widely applied as an oxidant under common advanced oxidation processes (AOPs) due to the high oxidation potential (2.5 – 3.1 V vs NHE and 1.8 – 2.7 V vs NHE respectively) [16]. The convenient production of $SO_4^{\cdot-}$ and $\cdot OH$ are generated by activation of peroxymonosulfate (PMS), persulfate (PS) or peroxydisulfate (PDS) via UV, heat, ultrasound, electrochemical means [17–21], where the process can be assisted or catalyzed using transition metals [21]. Although the efficiency of AOPs is high, there are some drawbacks such as the high concentration of PMS or PDS residuals in the treated wastewater [22,23]. PS and PMS have been reported to have acute toxicity, which could pose other hazards and induce secondary pollution [24,25]. Thus, an Advanced Reduction Processes (ARPs) by activating sulfite to generate highly reductive radicals has been proposed as an alternative method [26]. Comparing with PMS and PDS, sulfite has been considered as a cheap, efficient, and eco-friendly chemical for the degradation of emerging organics. The activation could be done by UV, high energy electron beam (HEEB), ultrasound and microwave [27]. It has been reported that the application of heavy metal – Co (III) for the activation of sulfite may contribute to significant drawbacks such as the leaching of heavy metals into water [28]. Nonetheless, the direct activation by UV irradiation was found to be the most effective method for persistent compounds [29,30]. Thus, the application of UV to activate sulfite has been proposed by previous studies as a green technology to degrade emerging pollutants in water [16].

UV/sulfite process has demonstrated excellent performance on the removal of organic pollutants and heavy metals by providing exclusive reducing and oxidizing agents [31,32]. It has been reported that the photolysis of sulfite can generate reductive species such as hydrated electrons (e_{aq}^-, $-2.9 V vs. NHE$), Hydrogen radical ($H^\bullet$, $-2.3 V vs. NHE$) and sulfite anion radicals ($SO_3^{\bullet-}$, $0.63 - 0.84$ V) [33–35]. The e_{aq}^- has been reported as a nucleophile that can react with organic molecules by attaching to aromatic rings or substituting one electron on alkene double bonds [36]. Meanwhile, it has been demonstrated that the $SO_3^{\bullet-}$ can further dissociate with dissolved oxygen (DO) in water to produce extra oxidizing agents ($SO_5^{\cdot-}$, $SO_4^{\cdot-}$ and $\cdot OH$) which can initiate AOPs [37–40].

Despite the high efficiencies for both AOPs and ARPs, the studies on the discovery of this ARP/AOP hybrid system was currently limited. Thus, the aim of this study is to examine the performance of UV/sulfite for the removal of DPH, as well as investigating the synergetic effects of combined AOP/ARP. Various parameters were investigated for process optimization and the degradation mechanisms were studied via the identification of the reaction pathways.

2. Methodology

2.1. Chemicals and reagents

All chemicals are analytic reagent grade and all solvents and HPLC or LCMS grade and were used as received without further purification. Diphenhydramine Hydrochloride (99 %, $C_{17}H_{22}ClNO$) was purchased from Acros Organics, USA. Sodium Sulfite (98 %, Na_2SO_3) was purchased from BDG Laboratory Supplies, England. Acetonitrile, Methanol

and $Na_2S_2O_3$ (99 %) where purchased from Duksan. NaOH and HCl were used for pH adjustment and were purchased from Sigma-aldrich. Anions (Na_2SO_4, $NaHCO_3$, $NaNO_2$, $NaNO_3$ and NaCl) were purchased from Riedel-deHaen.

2.2. Experimental procedures

The photodegradation was carried out in a UV reactor installed with three UV lamps and a mixer. The experimental setup is shown in **Fig. S1**. The UV lamps were turned on 20 min prior the experiment to ensure stable UV light intensity. The mixer was in fixed position to ensure homogeneity throughout the reaction process. The pH of reaction mixture was adjusted by HCl or NaOH. 750 uL of sample was extracted from the suspension in specific operating time interval and was immediately quenched by 250 μL of methanol. For TOC measurement, 8 mL of sample was mixed with 12 mL of sodium thiosulfate quencher to prevent any interference.

2.3. Analytical methods

The concentration of DPH in samples were quantified by HPLC consisting of a Waters 2487 pump and a Waters Symmetry column (4.6 × 150 mm, 5 μm particle size), with a flow rate of 1.0 mL/ min with 80 μL injection volume. The detection wavelength was set at 220 nm. The mobile phase was a mixture acetonitrile and water at 60:20 (v/v) with 0.1 % phosphoric acid. TOC measurement was performed using TOC-L analyzer purchased from Shimadzu TOC 5000A equipped with an ASI-5000A autosampler. The identification of reaction intermediates was conducted by Thermo Scientific Orbitrap Fusion Lumos Mass Spectrometer with ESI ion source at both positive and negative mode. The Orbitrap resolution is 120,000 and scan range is 50–500 m/z. The chromatography was conducted with a Waters Dionex UltiMate 3000 RSLCnano. The mobile phase is a mixture of A: water and B: acetonitrile. The gradient progressed linearly from 95 % A to 5 % from 0 to 9 min, and maintained at 5 % for 2 mins, and returned to initial condition in 0.5 min and maintained for 3 mins. The flow rate was 0.3 mL/min and the whole program lasts for 15 mins.

3. Results and discussions

3.1. Effect of UV wavelengths

Two sets of experiments were conducted under different wavelengths with same initial [DPH] at 0.05 mM with and without sodium sulfite to reveal the effect of direct photolysis and UV/sulfite at different UV wavelengths and the result is shown in **Fig. 1**. In general, experiments with sodium sulfite performed better than direct photolysis where 254 nm/sulfite has the best performance among all, with complete removal in 6 min. Without sulfite, the removal of DPH by direct photolysis was very limited. For 254 nm, the removal of DPH by direct photolysis is around 15 %, which is noticeably higher than 300 and 350 nm (5 % and 1 %). This is because shorter wavelength can provide higher photon energy which more $SO_3^{\bullet-}$ can be activated from sulfite. With the addition of sulfite, the removal of DPH at 300 nm and 350 nm has only increased slightly (5 % and 8 % respectively). However, the removal of DPH has reached 100 % at 254 nm which is significantly better then UV_{300} and UV_{350}. Despite the higher photon energy provided at 254 nm, it has been demonstrated that the molar extinction coefficient of sulfite is significant only at wavelength below 260 nm [41]. Moreover, the absorptivity of sulfite has been reported to drop from 3.0 to zero when wavelength is greater than 260 nm [42]. Thus, the activation of sulfite by UV at 300 nm and 350 nm are very limited. The significantly better performance of UV_{254}/sulfite can be attributed to both improved photolysis and the efficient activation of sulfite to produce reactive radicals for DPH degradation as shown in **Eq. (1) – (5)** [38–40,43]. Apart from the production of $SO_3^{\bullet-}$ and e_{aq}^- by photolysis,
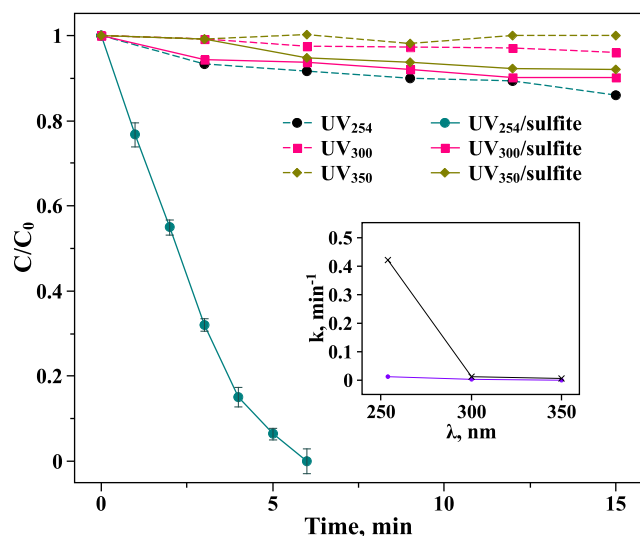
Fig. 1. Effect of UV wavelengths with and without sodium sulfite. *Experimental Condition:* $[DPH]_0 = 0.010$ mM; $[sulfite]_0 = 1.0$ mM; pH = 7.8.

$SO_3^{\bullet-}$ can also react with dissolved oxygen in water to form $SO_5^{\bullet-}$, with $SO_5^{\bullet-}$ to produce $SO_4^{\bullet-}$ by reacting with $SO_3^{\bullet-}$ and self-scavenging.

$$SO_3^{2-} \xrightarrow{h\nu} SO_3^{\bullet-} + e_{aq}^- \tag{1}$$

$$SO_3^{\bullet-} + O_2 \rightarrow SO_5^{\bullet-} \tag{2}$$

$$SO_5^{\bullet-} + SO_5^{\bullet-} \rightarrow O_2 + 2SO_4^{\bullet-} \tag{3}$$

$$SO_5^{\bullet-} + SO_3^{2-} \rightarrow SO_4^{2-} + SO_4^{\bullet-} \tag{4}$$

$$SO_4^{\bullet-} + H_2O \rightarrow H^+ + SO_4^{2-} + HO^{\bullet} \tag{5}$$

Since UV$_{254}$/sulfite has a desirable performance on DPH degradation, this process was selected for other experiments in this study.

3.2. Effect of sulfite dosage

To evaluate the influence of sulfite on DPH degradation, different dosages of sodium sulfite ranging from 0.1 to 5.0 mM were tested as
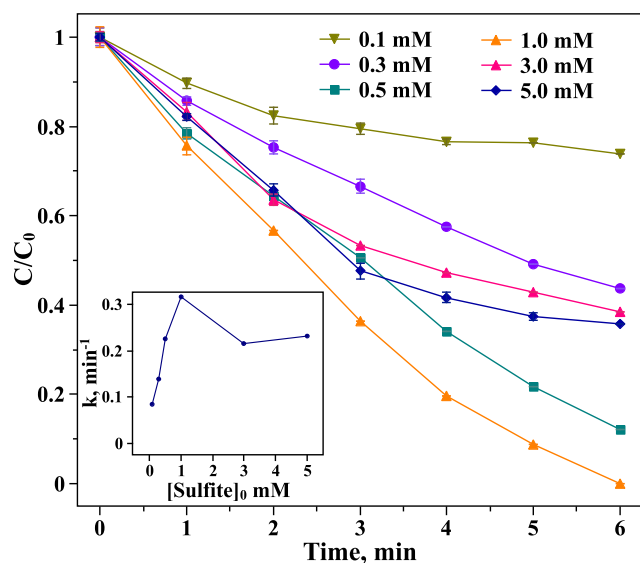
Fig.2. Effect of sulfite dosage. *Experimental Condition:* $[DPH]_0 = 0.010$ mM; pH = 7.8; UV lamps at 254 nm were employed.

shown in Fig. 2. From $[Sulfite]_0$ 0.1 to 1.0 mM, the degradation rate and removal increased linearly. Both the reaction rate and removal are optimal at $[Sulfite]_0 = 1.0$ mM. According to the decay rate constants at different $[sulfite]_0$, a linear relationship was proposed when $[sulfite]_0$ is less than 1.0 mM (**Eq. (6)**). The increase in SO_3^{2-} supply could lead to more production of reactive radicals such as e_{aq}^- and $SO_3^{\bullet-}$ via **Eq. (6)** for DPH degradation. However, when $[sulfite]_0$ is further increased beyond its optimal, a decline in reaction rate and removal was observed. One possible explanation for this phenomenon is that an overdose of sulfite could hinder the average UV light intensity adsorbed by the solution [44], where the activation of sulfite could be reduced. Apart from the blockage of UV light, the self-scavenging effect of $SO_3^{\bullet-}$ can also hinder the reaction as less radicals are available for reaction (**Eq. (7) – (8)**) [45]. It is also reported that e_{aq}^- can form an adduct with sulfite ions (**Eq. (9)**) [46], reducing the amount of e_{aq}^- for reaction. To minimize the scavenging effect, the concentration of sodium sulfite added to the reaction should be controlled to maintain the optimal sulfite radical quantity. In this case, $[sulfite]_0 = 1.0$ mM was adopted for all the other tests.

$$k = 0.26[sulfite]_0 + 0.07, \ when \ [sulfite]_0 \leqslant 1.0 \ mM \tag{6}$$

$$SO_3^{\bullet-} + SO_3^{\bullet-} \rightarrow S_2O_6^{2-} \tag{7}$$

$$SO_3^{\bullet-} + SO_3^{\bullet-} + H_2O \rightarrow SO_4^{2-} + HSO_3^- + H^+ \tag{8}$$

$$e_{aq}^- + SO_3^{2-} - \rightarrow HSO_3^{2-} + OH - \tag{9}$$
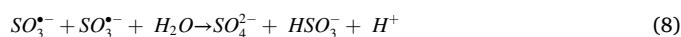
3.3. Effect of anions

It has been reported that the photochemical activities of inorganic anions in water may affect the removal of organics in UV/sulfite system [35,47]. The anions that can influence the UV/sulfite system include NO_3^-, NO_2^-, Cl^-, HCO_3^-, and SO_4^{2-}. Thus, these anions were selected in this study to evaluate their effect on UV/sulfite process.

As shown in Fig. 3a – 3b, only the addition of NO_3^- have positive effect on the UV/sulfite process, resulting in a faster initial decay rate ($k = 0.138$ min^{-1}). However, the final removal of DPH was then hindered after 10 min. The increase of initial rate could be due to the photolysis of NO_3^- which extra oxidizing agents $O(^3P)$ and $HO^{\bullet}$ generated (**Eq. (10) – (12)**). The reduced DPH removal could be due to the NO_3^- scavenging effect on e_{aq}^- which reduced the overall reactive species in the system (**Eq. (13)**).

$$NO_3^- \xrightarrow{h\nu} NO_2^- + O(^3P) \tag{10}$$

$$NO_3^- \xrightarrow{h\nu} NO_2^{\bullet} + O^{\bullet-} \tag{11}$$

$$O^{\bullet-} + H_2O \rightarrow HO^{\bullet} + OH^- \tag{12}$$

$$NO_3^- + e_{aq}^- \rightarrow (NO_3^{\bullet})^{2-} \tag{13}$$

To further elaborate the effect of NO_3^- on DPH degradation, different dosages of NO_3^- (10 mM, 30 mM, and 60 mM) were examined under both UV/sulfite process and direct photolysis (Fig. 3c – 3d). According to Fig. 3c, increasing the dosage of NO_3^- to 60 mM has neither increased the initial decay rate, nor hindered the final removal comparing with 10 mM dosage. This means that the production of reaction species (**Eq. (10) – (12)**) and reduction of reaction species (**Eq. (13)**) is approaching equilibrium, which higher dosage will not significantly increase nor reduce functional reaction species. According to Fig. 3d, increasing the dosage of NO_3^- from 10 mM to 60 mM can result in an increase on both reaction rate and final removal under direct photolysis without sulfite. This can convince that the photolysis of NO_3^- has provided extra reaction species into the degradation system and has
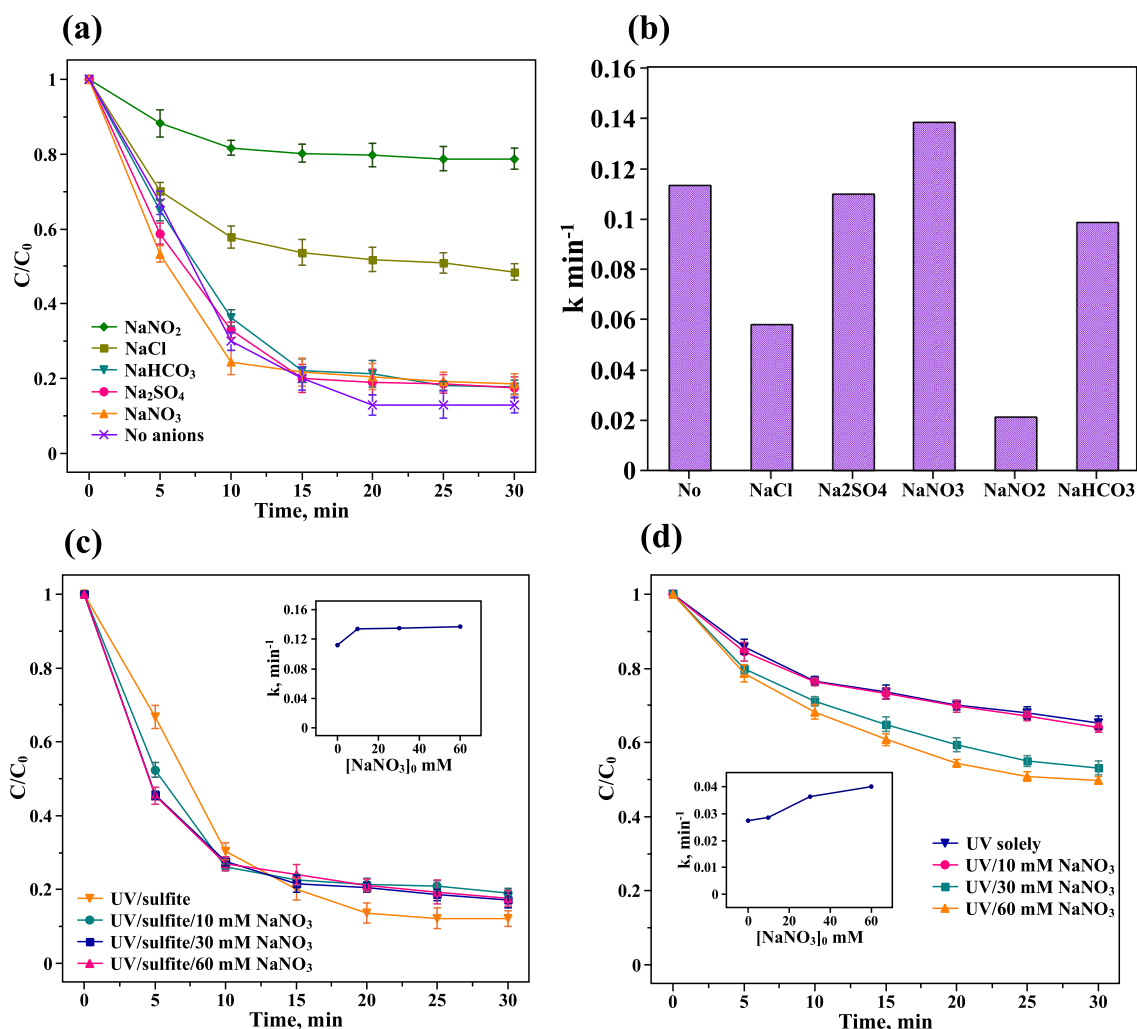
Fig.3. **(a)** Effect of anions; **(b)** The rate constants in the presence of different anions; **(c)** Effect of NaNO₃ in UV/sulfite process; **(d)** Effect of NaNO₃ using sole UV process. *Experimental Condition:* [DPH]$_0$ = 0.010 mM; [sulfite]$_0$ = 1.0 mM; pH = 7.8; UV lamps at 254 nm were employed.

scavenged the reaction species produced from sulfite.

All other studied anion species have reduced the reaction rate and removal capacity of UV/sulfite process. According to Fig. 3a, NO_2^- has retarded the system the most among all anions. Although NO_2^- can produce e_{aq}^- and $HO^•$ under photolysis (**Eq. (14) – (16)**), the $HO^•$ will then undergo diffusion control (**Eq. (17) – (18)**) to form other products with $NO^•$ or NO_2^-, which will significantly reduce the $HO^•$ produced. Moreover, NO_2^- has been reported to be an e_{aq}^- scavenger as shown in **Eq. (19)** [48]. This will reduce the reaction species in UV/sulfite system which resulted in strong process retardation. Comparing with Cl^- anions, the impact of HCO_3^- and SO_4^{2-} anions towards UV/sulfite process was minimal. The Cl^- anions have restricted the process because Cl^- can scavenge the $SO_4^{•-}$ and $HO^•$ produced from sulfite as shown in **Eq. (20) – (21)**. Besides, it has been reported that HCO_3^- can also scavenge $SO_4^{•-}$ and $HO^•$ with second-order rate constant of 1.6×10^6 $M^{-1} s^{-1}$ and $8.5 \times 10^6 M^{-1} s^{-1}$ respectively [49]. Thus, HCO_3^- anions also exhibited the ability to reduce the overall performance of UV/sulfite process.

$$NO_2^- \xrightarrow{hv} NO_2^• + e_{aq}^- \tag{14}$$

$$NO_2^- \xrightarrow{hv} NO^• + O^{•-} \tag{15}$$

$$O^{•-} + H_2O \rightarrow HO^• + OH^- \tag{16}$$

$$NO^• + HO^• \rightarrow HNO_2 \tag{17}$$

$$NO_2^- + HO^• \rightarrow NO_2^• + OH^- \tag{18}$$

$$NO^{2-} + \rightarrow (NO_2)^{2-} \tag{19}$$

$$Cl^- + SO_4^{•-} \rightarrow Cl^• + SO_2^{4-} \tag{20}$$

$$Cl^- + HO^• \rightarrow ClOH^{•-} \tag{21}$$
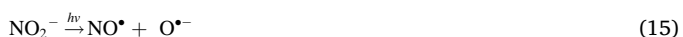
3.4. Effect of DPH dosage

The effect of initial DPH concentration was tested from 0.005 mM to 0.100 mM DPH as shown in Fig. 4a. Complete removal was achieved with DPH initial concentration lower than 0.010 mM. As the detected environmental DPH in stream is less than 0.0004 μM, the system is found to be useful for environmental DPH treatment. The removal and reaction rates decrease with increasing DPH concentration, suggesting that the sulfite is the liming factor, where the competition between DPH and radicals increases with [DPH]$_0$. Moreover, the increase in [DPH]$_0$ causes more production of intermediate compounds, which will also lead to competition for radicals, causing even slower reaction. For accurate prediction of the reaction performance, the correlation between the first order rate constant k and $1/[DPH]_0$ is shown in **Fig. 4b** and is expressed as **Eq. (22)**. The equation shows a straight-line correlation, indicating
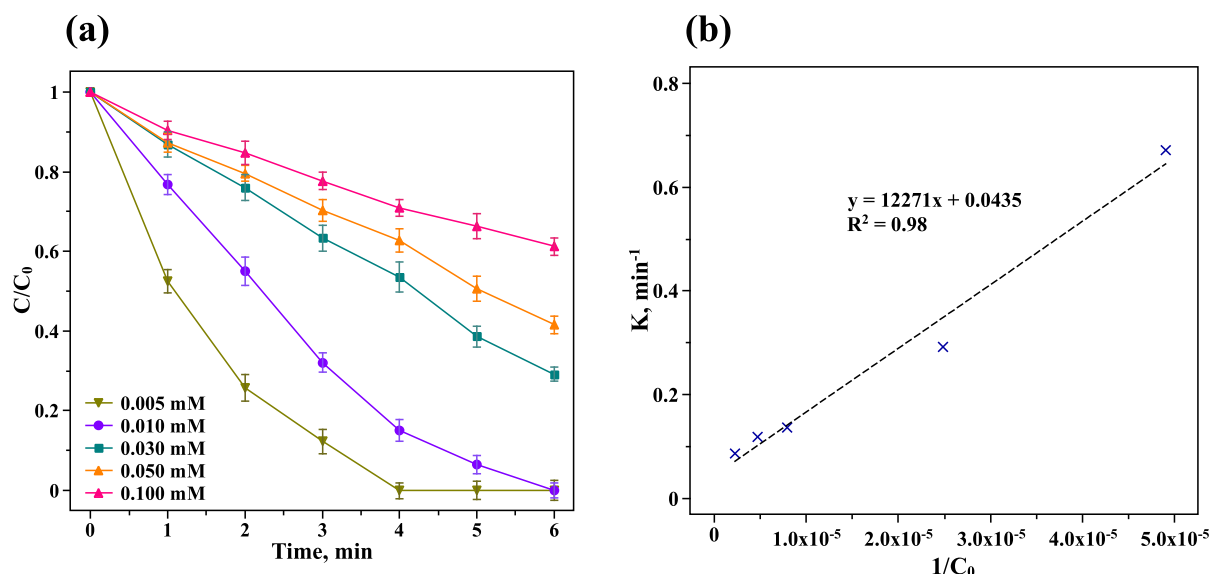
Fig.4. **(a)** Effect of initial DPH concentration and (b) Correlation between decay rate constants and [DPH]$_0$. *Experimental Condition:* [sulfite]$_0$ = 1.0 mM; pH = 7.8; UV lamps at 254 nm were employed.

that the reaction rate constant k is inversely proportional to [DPH]$_0$.

$$k = 0.003/[DPH]_0 + 0.079 \qquad (22)$$

3.5. Effect of initial pH under UV$_{254}$/Sulfite

The initial pH of the reaction solution is an important parameter for UV/sulfite degradation process as pH can affect the dominant species and the pathway of DPH removal. The initial pH level from 2.56 to 10.99 were studied under the UV$_{254}$/sulfite system. The results were shown in Fig. 5**a – b** and the dissociation of ion species varies at different pH are predicted and presented in Fig. 5**c.** According to Fig. 5**a**, it was noted that the optimum pH value for the removal of DPH was 10.04, which pH adjustments was required to achieve desired pH values for this system. The reaction rate in acidic pH (i.e. pH 2.7 to 5.6) was sluggish where only less than 30 % of DPH were removed within 30 min. According to Fig. 5**b**, although the optimum pH was observed to be 10.04, the pH during reaction was constant through the reaction. Instead, the pH has a significant drop at pH 5.12 to 7.86 which indicated that acidic reaction intermediates were tending to be produced under a more neutral condition. This is because the dissociation of H$^\bullet$ was the highest at pH 5.12 to 7.86 which can promote hydrogenation of intermediates to form –COOH compound. A summary of the reactions under acidic pH is listed in Table 1.

It was observed that the reaction rate and removal efficiency was significantly improved in alkaline pH condition comparing with acidic environment. This could be due to the variation on molar absorptivity of sulfite under UV irradiation with pH. It has been demonstrated that an increase in pH from 3 to 7 can cause the absorptivity to increase for more than 12 folds and further pH increment results in linear increase in absorptivity [27], such that the UV activation is more favorable at high pH.

Apart from the variation of molar absorptivity, the reaction was retarded at lower pH as the abundant H$^+$ in the acidic solution causes scavenging effect on e$^-_{aq}$ (**Eq. 23**) at $k = 2.3 \times 10^{10}$ M^{-1}s^{-1} [46], such

Table 1
Reactions in acidic pH.

Reactions	Favorable pH/ pKa	Eq.
e$^-_{aq}$+H$^+$ ⇌ H	Acidic / pKa = 9.7	(23)
SO$_3^{2-}$ + H$^+$ ⇌ HSO$_3^-$	pKa = 7.2	(24)
HSO$_3^-$ $\xrightarrow{h\nu}$ SO$_3^{\bullet-}$ + H$^\bullet$	Acidic	(25)
e$^-_{aq}$ + HSO$_3^-$ →H$^\bullet$ + SO$_3^{2-}$	Acidic	(26)
e$^-_{aq}$ + H$^+$ →H$^\bullet$	Acidic	(27)
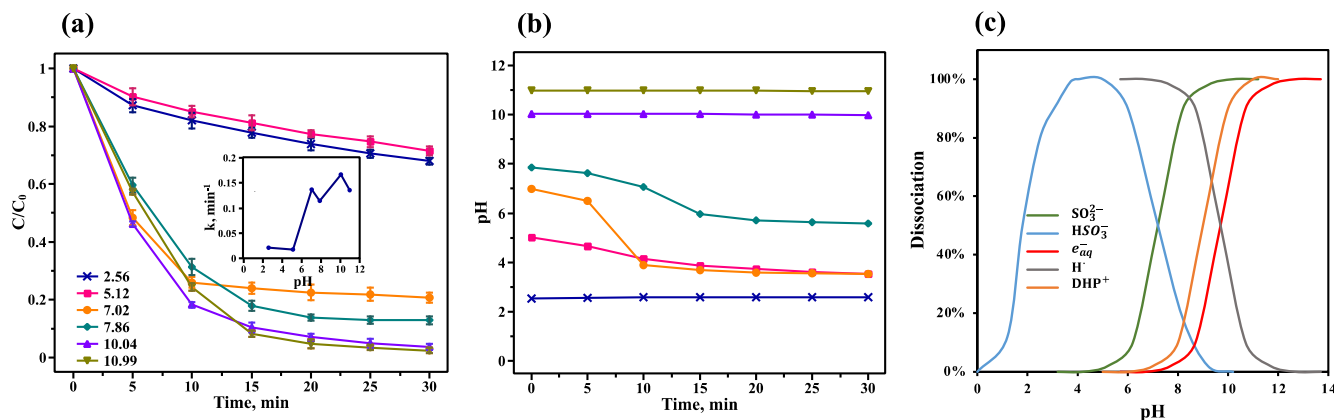
Fig. 5. **(a)** Effect of initial pH under UV/sulfite process **(b)** The evolution of pH during experiment **(c)** Theoretical dissociation of ion species at different pH levels. *Experimental Condition:* [DPH]$_0$: 0.05 mM; [sulfite]$_0$ = 1.00 mM; UV lamps at 254 nm were employed.

that less e_{aq}^- are available for reaction. It has been reported that the concentration of e_{aq}^- is at least 4 to 5 times more in pH 9 than pH 4 – 5 [50]. According to Fig. 5c, at pH less than 7.2, SO_3^{2-} tends to form HSO_3^- with H^+ in the solution (**Eq. 24**), which induced a shift of dominant species from SO_3^{2-} to HSO_3^-, where it has been reported that in pH 3, HSO_3^- accounts for more than 90 % and SO_3^{2-} for less than 10 % [51]. Although HSO_3^- can still be activated to form radicals (**Eq. 25**) [51], the reaction rate is much less than for SO_3^{2-} for a few reasons. First, the absorption coefficient of HSO_3^- has an onset at a shorter wavelength at around 210 nm, and under the studied UV wavelength (i.e. 254 nm), the absorption is almost four times less than that for SO_3^{2-} [50]. Also, the quantum yield of HSO_3^- under UV irradiation is halved compared to SO_3^{2-} [27]. Moreover, at acidic solution, abundant H^+ and predominant HSO_3^- ions act as scavengers for e_{aq}^- (**Eq. 26 – 27**), once again reducing the available e_{aq}^- for reaction. Altogether, the degradation by $SO_3^{\bullet-}$ and e_{aq}^- is hindered at lower pH, and since the removal is similar to photolysis presented earlier, the removal pathway at acidic pH is proposed to be solely direct photolysis.

At alkaline pH, the reaction is notably faster as the dissociation of SO_3^{2-} (**Eq. 24**) is favored at pH higher than the pKa of DPH (pKa = 8.87), which resulted in more available SO_3^{2-} for activation. It has been reported in previous study that at pH higher than 9, 98 % of sulfite are in the form of SO_3^{2-} [52], indicating that SO_3^{2-} is the dominant species in alkaline pH. At this pH range, the rate of photolysis, absorption coefficient and quantum yield for SO_3^{2-} is favored in this pH range, resulting 6 – 7 times faster reaction.

Moreover, it has been reported that in the presence of O_2, $SO_3^{\bullet-}$ can react together to form $SO_5^{\bullet-}$ with higher reduction potential ($E^\circ = -0.89$ V), which is much more powerful than $SO_3^{\bullet-}$ ($E^\circ = -0.72$ V) [53] (**Eq. (2)**). This phenomenon occurs mainly only in alkaline pH, which $SO_5^{\bullet-}$ further propagates to form even more powerful $SO_4^{\bullet-}$ and $OH^\bullet$ by self-combination (**Eq. (3)**) or by reaction with SO_3^{2-} (**Eq. (4) & (5)**) [54]. At this stage, the synergetic effect of combined advanced oxidation and reduction (AOP/ARP) was observed. The AOP/ARP process can provide extra degradation pathway for DPH including hydroxylation, cleavage of alkylate side chain and loss of aromatic ring, resulting at a much better performance than in lower pH. Thus, the optimum for this reaction will occur at pH 10.04 as the production of $SO_4^{\bullet-}$ and $SO_5^{\bullet-}$ is favored. According to Fig. 5c, the dissociation of e_{aq}^- (**Eq. 23**) can reach 100 % at pH 10.04 which can contribute to the notable increase in reaction rate as the standard reduction potential of e_{aq}^- ($E^\circ = -2.77$ V) is higher than $H^\bullet$ ($E^\circ = -2.42$ V) [55]. The e_{aq}^- can also reacts with dissolved oxygen to form another radical, $O_2^{\bullet-}$ (**Eq. 28**) [56], which is proposed to contribute considerably to the increased rate. Apart from that, the DPH will be protonated to form DPH^+ ions with pH > pKa (**Eq. 29**), which can also contribute to faster degradation of probe compound. The reactions involved in alkaline solution are summarized in Table 2.

To further elaborate the impact of pH on DPH degradation with UV and sulfite in aqueous condition, the degradation of DPH by solely photolysis (**Fig. S2a**), solely sulfite (**Fig. S2b**) and solely hydrolysis

(**Fig. S2c**) under various pH was examined. The results indicated that the reaction would be retarded at neutral pH for the three comparative tests which indicated that the dissociation of e_{aq}^- and DHP^+ would affect the UV/sulfite process more significantly. In short, the UV/sulfite system for DPH degradation is significantly more efficient in alkaline pH due to physical (molar absorptivity, quantum yield), chemical (dissociation of desired ions at higher pH) properties and the combined effects of AOP/ARP.

3.6. Role of radical species in the UV/sulfite system

As the activation of sulfite can be achieved by adopting UV_{254} irradiation, leading to the generation of the sulfite anion radicals ($SO_3^{\bullet-}$), aqueous electron (e_{aq}^-), and other oxidizing radicals ($SO_4^{\bullet-}$ & $OH^\bullet$) under aerobic conditions (**Eq. (2) – (3)**) [38,54,57]. Therefore, it is vital to investigate the dominating reactive species for the DPH degradation in the UV_{254}/sulfite process. To examine the reaction mechanism, different types of scavengers were added to the reactions. Five types of scavengers, NO_2^-, NO_3^-, methanol, butanol and nitrogen purging were added into separate solutions as shown in Fig. 6. It is concluded that except for NO_3^-, the addition of all other four kinds of scavengers caused a decline in removal in different degrees. The order of retardation in terms of reaction rate is summarized as $NO_2^- >$ Methanol > Butanol > $N_2 > NO_3^-$.

Interestingly, the removal of oxygen via nitrogen purging did not cause a complete retardation, where only 38 % of decline in the degradation efficiency was observed. It is anticipated that the production of powerful reactive species such as $SO_4^{\bullet-}$ and $OH^\bullet$ will be hindered in the absence of oxygen (**Eq. (2) – (3)**), implying that the DPH degradation can be achieved using $SO_3^{\bullet-}$ and/or e_{aq}^-. The addition of NO_3^- did not cause a notable effect on the degradation efficiency, which is unexpected due to the high capability of NO_3^- to scavenge e_{aq}^- (**Eq. (13)**) [26,49]. Instead, the presence of NO_3^- resulted in a positive effect on the degradation rate with about 20 % increment in rate constant during the first 10 min. This could be rationalized by two reasons: (1) the direct photolysis of NO_3^- at UV_{254} produced new powerful reactive radicals (**Eq. (10) – (12)**) [58] and (2) the dominating role of $SO_3^{\bullet-}$ in the DPH degradation. To further reveal the role of e_{aq}^- in the degradation mechanism, NO_2^- was also applied as a scavenger for e_{aq}^- (**Eq. (19)**) [48]. The addition of NO_2^- showed the highest retardation effect on the DPH degradation among the five tests where the degradation is even slightly less than direct photolysis. This result suggested that the contribution of e_{aq}^- to the DPH degradation efficiency was minimal at pH 8.1 as the dissociation of e_{aq}^- at pH 8.1 was unsignificant.

To explore the role of $SO_4^{\bullet-}$ and $OH^\bullet$, methanol and *tert*-butanol alcohols were utilized as scavengers for $SO_4^{\bullet-}$ and $OH^\bullet$. Methanol can quench both $SO_4^{\bullet-}$ and $OH^\bullet$ at higher efficiency ($k_2(SO_4^{\bullet-}) = 0.9$–$1.3 \times 10^7$ M^{-1} s^{-1}, $k_2(OH^\bullet) = 0.8$–1.0×10^9 M^{-1} s^{-1}) [26,49,59] while *tert*-butanol can effectively quench $OH^\bullet$ only ($k_2(SO_4^{\bullet-}) = 4.0$–$9.1 \times 10^5$ M^{-1} s^{-1}, $k_2(OH^\bullet) = 3.8$–7.6×10^8 M^{-1} s^{-1}) [26,59,60]. Conversely, the reactivity of $SO_3^{\bullet-}$ and $SO_5^{\bullet-}$ was reported to be low toward methanol and

Table 2
Reactions in alkaline pH.

Reactions	Favorable pH/ pKa	Eq
$SO_3^{\bullet-} + O_2 \rightarrow SO_5^{\bullet-}$	Alkaline	(2)
$SO_5^{\bullet-} + SO_5^{\bullet-} \rightarrow 2\,SO_4^{\bullet-} + O_2$	–	(3)
$SO_5^{\bullet-} + SO_3^{2-} \rightarrow SO_4^{\bullet-} + SO_4^{2-}$	–	(4)
$SO_4^{\bullet-} + H_2O \rightarrow SO_4^{2-} + H^+ + OH^\bullet$		(5)
$e_{aq}^- + O_2 \rightarrow O_2^{\bullet-}$	pH greater than 9	(28)
	pKa = 9	(29)
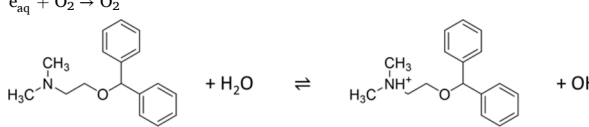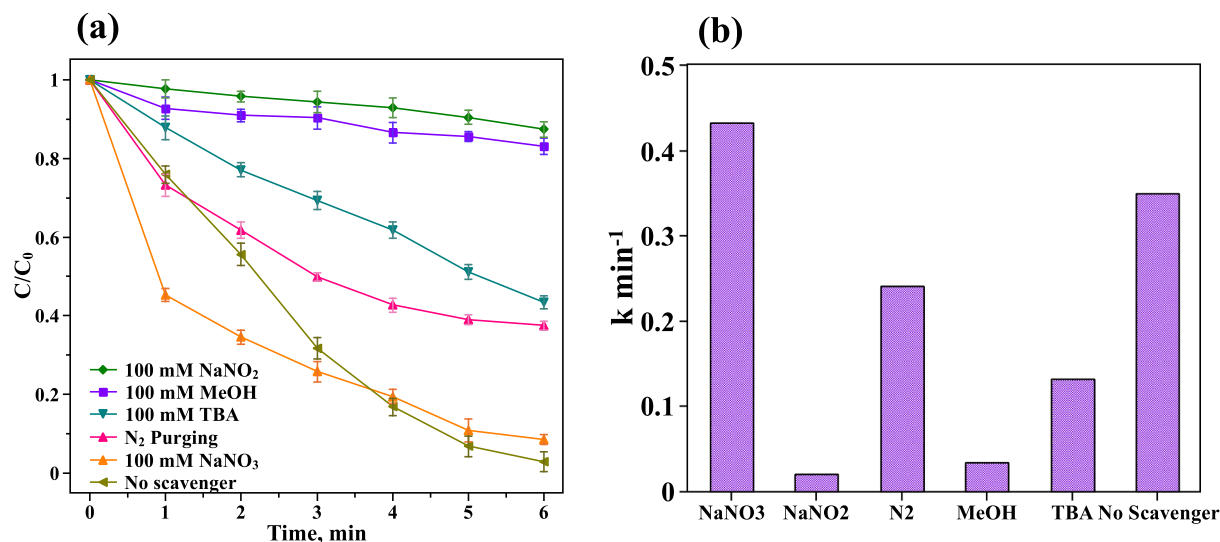
Fig. 6. (a) Effect of different scavengers on the degradation and **(b)** The rate constants at different scavengers. *Experimental Condition:* [DPH]$_0$: 0.010 mM; [sulfite]$_0$ = 1.0 mM; pH = 8.1; UV lamps at 254 nm were employed.

tert-butanol [26]. The results exhibited that methanol can significantly inhibit the degradation performance, whereas *tert*-butanol can minimize the decay efficiency by 40 %. The difference between adding methanol and butanol is considered to be the reaction by SO$_4^-$. In general, methanol and *tert*-butanol scavenging tests indicate the contribution of both SO$_4^{\bullet-}$ and OH$^\bullet$ to the DPH degradation efficiency. The overall results of scavenging tests showed that SO$_3^{\bullet-}$, SO$_4^{\bullet-}$, OH$^\bullet$ and e$_{aq}^-$ are the dominate reactive species responsible for the DPH decay in the UV$_{254}$/sulfite process suggesting the synergistic effect of both advanced reduction and advanced oxidation processes.

3.7. DPH degradation pathways

As illustrated in Scheme 1, a series of DPH degradation intermediates

formed from the UV photolysis of sulfite were traced and identified by the UPLC-ESI-MS system. All the intermediates were verified by comparing their obtained experimental *m/z* values with the corresponding mass spectrum in the LC/MS library (Table S1). Based on this technology, the DPH degradation was elucidated through four major pathways, including hydroxylation (A1-A4), cleavage of alkylamine side chain (B1-B6), loss of aromatic ring (C1-C5), and open of aromatic ring (D1-D4). These reaction products are considered to be involved in multiple chain reactions, which could be first being oxidized, then reduced, or *vice versa*.

Firstly, the hydroxylation was mediated by the OH$^\bullet$ radical addition on the aromatic ring with the loss of H$^\bullet$ to form A1, as OH$^\bullet$ are expected to be reactive towards electron rich aromatic systems by adducting on the meta-, ortho-, and *para*-positions [61]. The mono-hydroxylation
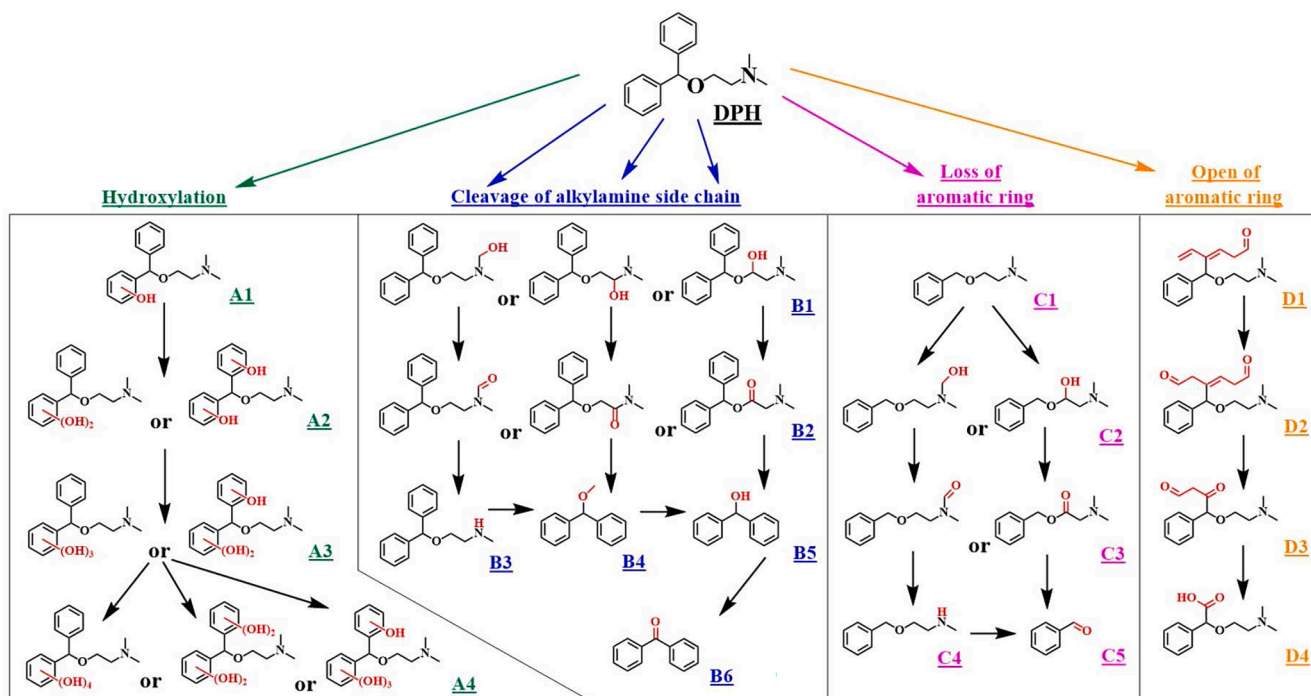
Scheme 1. Proposed DPH degradation pathways under UV/sulfite.

further increased the electron-rich property of phenyl ring, making it more readily to be di-hydroxylated [62]. While the addition of OH$^\bullet$ radicals on the other non-hydroxylated phenyl ring is another preferred way, which leads to the production of two mono-hydroxylated aromatic ring within a DPH molecule. Both constitutional isomers were grouped as intermediate A2. Likewise, A2 underwent a series of oxidation from the attack of reactive radicals to generate tri-hydroxylated A3 and tetra-hydroxylated A4, accordingly [63]. Secondly, the cleavage of alkyl-amine side chain is another possible way for DPH decay in the UV photolysis of sulfite. It was initiated by hydroxylation on different positions of alkylamine chain to give the birth of derivatives B1. The further oxidation occurred on different hydroxylated sites of B1 via H-abstraction reaction with OH$^\bullet$ and subsequently formed ketonic product B2 with several isomers. Afterwards, B3 was originated from a demethylation effect at N—C bond. B4 was assigned to the product of deamidation by $e^-_{aq}/SO_3^{\bullet-}$ reaction with amine group from B2 and the scission of amino group from B3. Further oxidation took place on B2 or B4 to yield diphenylmethanol (B5) through the dissociation of benzyl or the break of ketone group, respectively. The benzophenone fragments (B6) was emerged by the further transformation of B5 based on H-abstraction of $e^-_{aq}/SO_3^{\bullet-}$ [64]. Thirdly, as a parallel degradation route, DPH was found to loss one aromatic ring, yielding the derivative C1 which conserves single phenyl ring. Two isomers of derivative *C*2 could be assigned according to the OH$^\bullet$ radical electrophilic adduction on the alkylamine chain. The ketonic products (C3) were subsequently generated attributed to the H-abstraction on the hydroxyl group [65]. Further oxidation resulted in the scission of side chain on C3, generating C4 and C5 accordingly. Fourthly, the opening of aromatic ring in DPH structure was observed in the UV/sulfite process through the breakage of C=C bond in π orbitals, which give the birth of derivative D1 [66]. With the further attack of OH$^\bullet$ radicals, it is expected that the aliphatic chain of D1 was hydroxylated first and followed by the H-abstraction to produce ketonic structure D2 and D3, resulting in the scission of aliphatic chain. Carboxylation product was also observed from converting D3 to D4.

4. Conclusion

This study examined the mechanism of UV$_{254}$/sulfite for DPH degradation, and the process was able to achieve complete removal in 6 min under desirable pH levels. The pH level of solution was discovered to have greatly influenced the dominant species accounting for degradation. In summary, at lower pH, the reaction is hindered due to the dissociation of ineffective HSO_3^-, while at higher pH, SO_3^{2-} is the prevailing species, leading to the surge of reactive $SO_3^{\bullet-}$, $SO_4^{\bullet-}$ and e^-_{aq}, which contributed to the much faster degradation. The scavenging test has revealed that DPH can be degraded through both advanced oxidation and advanced reduction processes, where mainly $SO_3^{\bullet-}$, $SO_4^{\bullet-}$, OH$^\bullet$ and e^-_{aq} contributed to the degradation. It is discovered that among the five scavengers used, NO_3^- caused an increase in reaction rate due to the generation of an extra radical. The anions presented water will cause negative effect to the process. LCMS was also conducted to study the reaction pathway, and DPH was found to degrade into smaller molecules by H-abstraction, hydroxylation, side chain cleavage, losing aromatic ring or ring opening.

CRediT authorship contribution statement

Hiu Lam So: Writing – review & editing. **Liwen Wang:** Methodology, Investigation. **Jianghui Liu:** Visualization. **Wei Chu:** Conceptualization, Supervision, Funding acquisition. **Tao Li:** Formal analysis. **Amal Abdelhaleem:** Conceptualization, Methodology.

Declaration of Competing Interest

The authors declare that they have no known competing financial interests or personal relationships that could have appeared to influence the work reported in this paper.

Data availability

Data will be made available on request.

Appendix A. Supplementary material

Supplementary data to this article can be found online at https://doi.org/10.1016/j.seppur.2022.122193.

References

[1] K.-K. Oh, M. Adnan, D.-H. Cho, Network Pharmacology Study to Elucidate the Key Targets of Underlying Antihistamines against COVID-19, Current Issues Mol. Biol. 44 (2022) 1597–1609.

[2] L.R. Reznikov, M.H. Norris, R. Vashisht, A.P. Bluhm, D. Li, Y.-S.-J. Liao, A. Brown, A.J. Butte, D.A. Ostrov, Identification of antiviral antihistamines for COVID-19 repurposing, Biochem. Biophys. Res. Commun. 538 (2021) 173–179.

[3] J.P. Berninger, B. Du, K.A. Connors, S.A. Eytcheson, M.A. Kolkmeier, K.N. Prosser, T.W. Valenti, C.K. Chambliss, B.W. Brooks, Effects of the antihistamine diphenhydramine on selected aquatic organisms, Environ. Toxicol. Chem. 30 (2011) 2065–2072.

[4] B. Du, A.E. Price, W.C. Scott, L.A. Kristofco, A.J. Ramirez, C.K. Chambliss, J. C. Yelderman, B.W. Brooks, Comparison of contaminants of emerging concern removal, discharge, and water quality hazards among centralized and on-site wastewater treatment system effluents receiving common wastewater influent, Sci. Total Environ. 466–467 (2014) 976–984.

[5] P.E. Stackelberg, E.T. Furlong, M.T. Meyer, S.D. Zaugg, A.K. Henderson, D. B. Reissman, Persistence of pharmaceutical compounds and other organic wastewater contaminants in a conventional drinking-water-treatment plant, Sci. Total Environ. 329 (2004) 99–113.

[6] I. Ferrer, C.E. Heine, E.M. Thurman, Combination of LC/TOF-MS and LC/Ion Trap MS/MS for the Identification of Diphenhydramine in Sediment Samples, Anal. Chem. 76 (2004) 1437–1444.

[7] A.J. Ramirez, R.A. Brain, S. Usenko, M.A. Mottaleb, J.G. O`Donnell, L.L. Stahl, J. B. Wathen, B.D. Snyder, J.L. Pitt, P. Perez-Hurtado, L.L. Dobbins, B.W. Brooks, C. K. Chambliss, Occurrence of pharmaceuticals and personal care products in fish: Results of a national pilot study in the united states, Environ. Toxicol. Chem. 28 (2009) 2587–2597.

[8] A.J. Ramirez, M.A. Mottaleb, B.W. Brooks, C.K. Chambliss, Analysis of Pharmaceuticals in Fish Using Liquid Chromatography-Tandem Mass Spectrometry, Anal. Chem. 79 (2007) 3155–3163.

[9] S.N. Zhou, K.D. Oakes, M.R. Servos, J. Pawliszyn, Application of Solid-Phase Microextraction for In Vivo Laboratory and Field Sampling of Pharmaceuticals in Fish, Environ. Sci. Technol. 42 (2008) 6073–6079.

[10] Y. Chen, C. Hu, X. Hu, J. Qu, Indirect Photodegradation of Amine Drugs in Aqueous Solution under Simulated Sunlight, Environ. Sci. Technol. 43 (2009) 2760–2765.

[11] S.J. Wolfson, A.W. Porter, T.S. Villani, J.E. Simon, L.Y. Young, The antihistamine diphenhydramine is demethylated by anaerobic wastewater microorganisms, Chemosphere 202 (2018) 460–466.

[12] N. López, S. Plaza, A. Afkhami, P. Marco, J. Giménez, S. Esplugas, Treatment of Diphenhydramine with different AOPs including photo-Fenton at circumneutral pH, Chem. Eng. J. (Lausanne Switzerland 318 (2017) 112–120.

[13] Z. Li, P.-H. Chang, W.-T. Jiang, J.-S. Jean, H. Hong, L. Liao, Removal of diphenhydramine from water by swelling clay minerals, J. Colloid Interface Sci. 360 (2011) 227–232.

[14] R.P. Smith, R.E. Gosselin, J.A. Henderson, D.M. Anderson, Comparison of the adsorptive properties of activated charcoal and alaskan montmorillonite for some common poisons, Toxicol. Appl. Pharmacol. 10 (1967) 95–104.

[15] L. Song, C. Yi, Q. Wu, Z. Li, W. Zhang, H. Hong, Photocatalytic degradation of diphenhydramine in aqueous solution by natural dolomite, RSC Adv. 10 (63) (2020) 38663–38671.

[16] Y. Huang, C. Han, Y. Liu, M.N. Nadagouda, L. Machala, K.E. O'Shea, V.K. Sharma, D.D. Dionysiou, Degradation of atrazine by ZnxCu1−xFe2O4 nanomaterial-catalyzed sulfite under UV–vis light irradiation: Green strategy to generate SO4, Appl. Catal. B, Environ. 221 (2018) 380–392.

[17] X. He, A.A. de la Cruz, D.D. Dionysiou, Destruction of cyanobacterial toxin cylindrospermopsin by hydroxyl radicals and sulfate radicals using UV-254nm activation of hydrogen peroxide, persulfate and peroxymonosulfate, J. Photochem. Photobiol. A, Chem. 251 (2013) 160–166.

[18] M.G. Antoniou, A.A. de la Cruz, D.D. Dionysiou, Degradation of microcystin-LR using sulfate radicals generated through photolysis, thermolysis and e − transfer mechanisms, Appl. Catal. B, Environ. 96 (3-4) (2010) 290–298.

[19] W. Chu, Y.R. Wang, H.F. Leung, Synergy of sulfate and hydroxyl radicals in UV/S2O82−/H2O2 oxidation of iodinated X-ray contrast medium iopromide, Chem. Eng. J. 178 (2011) 154–160.

[20] W.-S. Chen, Y.-C. Su, Removal of dinitrotoluenes in wastewater by sono-activated persulfate, Ultrason. Sonochem. 19 (2012) 921–927.

[21] H.L. So, W. Chu, Y.H. Wang, Naphthalene degradation by Fe2+/Oxone/UV - Applying an unconventional kinetics model and studying the reaction mechanism, Chemosphere 218 (2019) 110–118.

[22] H. Lin, J. Wu, H. Zhang, Degradation of clofibric acid in aqueous solution by an EC/Fe3+/PMS process, Chem. Eng. J. (Lausanne Switzerland 244 (2014) (1996) 514–521.

[23] C. Cai, J. Liu, Z. Zhang, Y. Zheng, H. Zhang, Visible light enhanced heterogeneous photo-degradation of Orange II by zinc ferrite (ZnFe2O4) catalyst with the assistance of persulfate, Sep. Purif. Technol. 165 (2016) 42–52.

[24] C. Liang, C.-W. Wang, Assessing acute toxicity potential of persulfate ISCO treated water, Chemosphere 93 (2013) 2711–2716.

[25] T. Olmez-Hanci, I. Arslan-Alaton, D. Dursun, Investigation of the toxicity of common oxidants used in advanced oxidation processes and their quenching agents, J. Hazard. Mater. 278 (2014) 330–335.

[26] S. Wu, L. Shen, Y. Lin, K. Yin, C. Yang, Sulfite-based advanced oxidation and reduction processes for water treatment, Chem. Eng. J. 414 (2021) 128872.

[27] V.S.V. Botlaguduru, B. Batchelor, A. Abdel-Wahab, Application of UV–sulfite advanced reduction process to bromate removal, J. Water Process Eng. 5 (2015) 76–82.

[28] Y. Zhang, W. Chu, Enhanced degradation of metronidazole by cobalt doped TiO2/sulfite process under visible light, Sep. Purif. Technol. 291 (2022) 120900.

[29] B.P. Vellanki, B. Batchelor, Perchlorate reduction by the sulfite/ultraviolet light advanced reduction process, J Hazard Mater 262 (2013) 348–356.

[30] B.P. Vellanki, B. Batchelor, A. Abdel-Wahab, Advanced Reduction Processes: A New Class of Treatment Processes, Environ. Eng. Sci. 30 (5) (2013) 264–271.

[31] Z. Ren, U. Bergmann, T. Leiviskä, Reductive degradation of perfluorooctanoic acid in complex water matrices by using the UV/sulfite process, Water Res. 205 (2021) 117676.

[32] B. Xie, C. Shan, Z. Xu, X. Li, X. Zhang, J. Chen, B. Pan, One-step removal of Cr(VI) at alkaline pH by UV/sulfite process: Reduction to Cr(III) and in situ Cr(III) precipitation, Chem. Eng. J. 308 (2017) 791–797.

[33] B.F. Bachman, D.i. Zhu, J. Bandy, L. Zhang, R.J. Hamers, Detection of Aqueous Solvated Electrons Produced by Photoemission from Solids Using Transient Absorption Measurements, ACS Measurem. Sci. Au 2 (1) (2022) 46–56.

[34] T.N. Das, R.E. Huie, P. Neta, Reduction potentials of SO3•-, SO5•-, and S4O6• 3-radicals in aqueous solution, J. Phys. Chem. A 103 (18) (1999) 3581–3588.

[35] S. Liu, Y. Fu, G. Wang, Y. Liu, Degradation of sulfamethoxazole by UV/sulfite in presence of oxygen: Efficiency, influence factors and mechanism, Sep. Purif. Technol. 268 (2021).

[36] G.V. Buxton, C.L. Greenstock, W.P. Helman, A.B. Ross, Critical Review of rate constants for reactions of hydrated electrons, hydrogen atoms and hydroxyl radicals (·OH/·O− in Aqueous Solution, J. Phys. Chem. Ref. Data 17 (1988) 513–886.

[37] P. Neta, E.H. Robert, Free-Radical Chemistry of Sulfite, Environ. Health Perspect. 64 (1985) 209–217.

[38] A. Abdelhaleem, W. Chu, X. Liang, Diphenamid degradation via sulfite activation under visible LED using Fe (III) impregnated N-doped TiO2 photocatalyst, Appl. Catal. B 244 (2019) 823–835.

[39] Y. Wei, Q. Zou, P. Ye, M. Wang, X. Li, A. Xu, Photocatalytic degradation of organic pollutants in wastewater with g-C3N4/sulfite system under visible light irradiation, Chemosphere 208 (2018) 358–365.

[40] G. Li, C. Wang, Y. Yan, X. Yan, W. Li, X. Feng, J. Li, Q. Xiang, W. Tan, F. Liu, H. Yin, Highly enhanced degradation of organic pollutants in hematite/sulfite/photo system, Chem. Eng. J. 386 (2020) 124007.

[41] D.P. Ames, J.E. Willard, Effect of Salt Concentration and Temperature on the Ultraviolet Absorption Spectra of Aqueous Thiosulfate and Sulfite, J. Am. Chem. Soc. 75 (1953) 3267–3268.

[42] L. Wang, Fast Degradation of Monochloroacetic Acid by BiOI-Enhanced UV/S(IV) Process: Efficiency and Mechanism, Catalysts 9 (2019) 460.

[43] A. Sheikhmohammadi, A. Yazdanbakhsh, G. Moussavi, A. Eslami, M. Rafiee, M. Sardar, M. Almasian, Degradation and COD removal of trichlorophenol from wastewater using sulfite anion radicals in a photochemical process combined with a biological reactor: Mechanisms, degradation pathway, optimization and energy consumption, Process Saf. Environ. Prot. 123 (2019) 263–271.

[44] X. Liu, S. Yoon, B. Batchelor, A. Abdel-Wahab, Degradation of vinyl chloride (VC) by the sulfite/UV advanced reduction process (ARP): Effects of process variables and a kinetic model, Sci. Total Environ. 454–455 (2013) 578–583.

[45] Y. Gu, W. Dong, C. Luo, T. Liu, Efficient Reductive Decomposition of Perfluorooctanesulfonate in a High Photon Flux UV/Sulfite System, Environ. Sci. Technol. 50 (2016) 10554–10561.

[46] L. Dogliotti, E. Hayon, Flash photolysis study of sulfite, thiocyanate, and thiosulfate ions in solution, J. Phys. Chem. 72 (1968) 1800–1807.

[47] L. Xu, Y. Sun, L. Gan, J. Han, P. Wang, L. Yu, X. Mei, W. Li, B. Lyu, C. Pei, W. Chu, Utilization of photochemical circulation between NO3− and NO2− in water to degrade photoinert dimethyl phthalate: Influence of organic media and mechanism study, Appl. Catal. B 259 (2019).

[48] X. Li, J. Ma, G. Liu, J. Fang, S. Yue, Y. Guan, L. Chen, X. Liu, Efficient reductive dechlorination of monochloroacetic acid by sulfite/UV process, Environ. Sci. Technol. 46 (2012) 7342–7349.

[49] G.V. Buxton, C.L. Greenstock, W.P. Helman, A.B. Ross, Critical review of rate constants for reactions of hydrated electrons, hydrogen atoms and hydroxyl radicals (· OH/· O− in aqueous solution, J. Phys. Chem. Ref. Data 17 (1988) 513–886.

[50] M. Fischer, P. Warneck, Photodecomposition and Photooxidation of Hydrogen Sulfite in Aqueous Solution, J. Phys. Chem 100 (1996) 15111–15117.

[51] Y. Chu, L. Xu, L. Gan, W. Qiao, J. Han, X. Mei, H. Guo, W. Li, C. Pei, H. Gong, X. Guo, Efficient destruction of emerging contaminants in water by UV/S(IV) process with natural reoxygenation: Effect of pH on reactive species, Water Res 198 (2021) 117143.

[52] Q. Xiao, T. Wang, S. Yu, P. Yi, L. Li, Influence of UV lamp, sulfur(IV) concentration, and pH on bromate degradation in UV/sulfite systems: Mechanisms and applications, Water Res 111 (2017) 288–296.

[53] T.N. Das, R.E. Huie, P. Neta, Reduction Potentials of SO3 •-, SO5 •-, and S4O6 •3-Radicals in Aqueous Solution, J. Phys. Chem. A 103 (1999) 3581–3588.

[54] U. Deister, P. Warneck, Photooxidation of sulfite (SO32-) in aqueous solution, J. Phys. Chem 94 (1990) 2191–2198.

[55] P. Wardman, Reduction Potentials of One-Electron Couples Involving Free Radicals in Aqueous Solution, J. Phys. Chem. Ref. Data 18 (1989) 1637–1755.

[56] Z. Wu, C. Shang, D. Wang, S. Zheng, Y. Wang, J. Fang, Rapid degradation of dichloroacetonitrile by hydrated electron (eaq–) produced in vacuum ultraviolet photolysis, Chemosphere 256 (2020) 126994.

[57] Y. Gu, T. Liu, Q. Zhang, W. Dong, Efficient decomposition of perfluorooctanoic acid by a high photon flux UV/sulfite process: Kinetics and associated toxicity, Chem. Eng. J. 326 (2017) 1125–1133.

[58] Y. Wu, L. Bu, X. Duan, S. Zhu, M. Kong, N. Zhu, S. Zhou, Mini review on the roles of nitrate/nitrite in advanced oxidation processes: Radicals transformation and products formation, J. Cleaner Prod. 273 (2020) 123065.

[59] H. Eibenberger, S. Steenken, P. O'Neill, D. Schulte-Frohlinde, Pulse radiolysis and electron spin resonance studies concerning the reaction of SO4. cntdot.-with alcohols and ethers in aqueous solution, J. Phys. Chem. 82 (1978) 749–750.

[60] E. Hayon, A. Treinin, J. Wilf, Electronic spectra, photochemistry, and autoxidation mechanism of the sulfite-bisulfite-pyrosulfite systems. SO2-, SO3-, SO4-, and SO5-radicals, J. Am. Chem. Soc. 94 (1972) 47–57.

[61] G. Louit, S. Foley, J. Cabillic, H. Coffigny, F. Taran, A. Valleix, J.P. Renault, S. Pin, The reaction of coumarin with the OH radical revisited: hydroxylation product analysis determined by fluorescence and chromatography, Rad. Phys. Chem. 72 (2005) 119–124.

[62] D. Cui, A.M. Mebel, L.E. Arroyo-Mora, C. Zhao, A. De Caprio, K. O'Shea, Fundamental study of the ultrasonic induced degradation of the popular antihistamine, diphenhydramine (DPH), Water Res. 144 (2018) 265–273.

[63] T. Li, A. Abdelhaleem, W. Chu, W. Xu, Efficient activation of oxone by pyrite for the degradation of propanil: Kinetics and degradation pathway, J. Hazard. Mater. 403 (2021) 123930.

[64] J. Jeong, W. Song, W.J. Cooper, J. Jung, J. Greaves, Degradation of tetracycline antibiotics: Mechanisms and kinetic studies for advanced oxidation/reduction processes, Chemosphere 78 (2010) 533–540.

[65] T. Li, A. Abdelhaleem, W. Chu, S. Pu, F. Qi, J Zou, S-doped TiO2 photocatalyst for visible LED mediated oxone activation: Kinetics and mechanism study for the photocatalytic degradation of pyrimethanil fungicide, Chem. Eng. J. 411 (2021), 128450.

[66] N. López, P. Marco, J. Giménez, S. Esplugas, Photocatalytic diphenhydramine degradation under different radiation sources: Kinetic studies and energetic comparison, Appl. Catal., B, 220 (2018) 497–505.